

# Directional Semantic Grasping of Real-World Objects: From Simulation to Reality

Shariq Iqbal Jonathan Tremblay Thang To Jia Cheng Erik Leitch  
Andy Campbell Kirby Leung Duncan McKay Stan Birchfield  
NVIDIA

**Abstract**—We present a deep reinforcement learning approach to grasp semantically meaningful objects from a particular direction. The system is trained entirely in simulation, with sim-to-real transfer accomplished by using a simulator that models physical contact and produces photorealistic imagery with domain randomized backgrounds. The system is an example of end-to-end (mapping input monocular RGB images to output Cartesian motor commands) grasping of objects from multiple pre-defined object-centric orientations, such as from the side or top. Coupled with a real-time 6-DoF object pose estimator, the eye-in-hand system is capable of grasping objects anywhere within the graspable workspace. Results are shown in both simulation and the real world, demonstrating the effectiveness of the approach.<sup>1</sup>

## I. INTRODUCTION

Recent research has made substantial progress in addressing the indiscriminate grasping problem, in which a robot learns to grasp any of several objects from a cluttered bin [1], [2], [3], [4]. In such approaches, it does not matter *which* object is grasped, only *that* one or more objects are grasped. These methods tend to be restricted to top-down grasping, in which the robot reaches down into a bin using an overhead camera for sensing.

More recent work has addressed the problem of *semantic grasping*, in which a robot learns to grasp a specific type of object—indicated by the user—from a cluttered bin [5]. Although such approaches address the question of *which* object to grasp, they do not address the question of *how* to grasp the objects, *i.e.*, the part of the object and direction of the grasp. Moreover, these methods are restricted to top-down grasping using overhead sensing.

In this paper, we take the next logical step and address the problem of grasping specific objects from specific directions. For many real-world tasks, the manner in which the object is grasped is important. To place one object adjacent to another, for example, a top-down grasp may be insufficient, because it would cause the end effector to collide with the other object during placement; rather, a side grasp (on the opposite side) is needed. In such cases, grasping objects in a specific manner, from a specific direction, is crucial. We refer to this problem as *directional semantic grasping*.

Work was performed while the first author, who is also affiliated with the University of Southern California, was an intern with NVIDIA. Email: shariqiqbal2810@gmail.com, {jtremblay, sbirchfield}@nvidia.com

<sup>1</sup>Video is at <https://youtu.be/bjJLtnDv9w>.

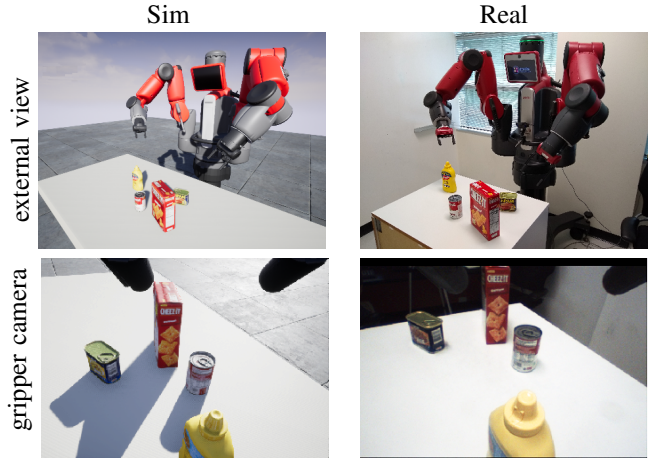


Fig. 1. We have developed a simulator that models physical contact and produces photorealistic imagery. The goal of this work is to learn a policy in simulation (left) that transfers to the real world (right) for grasping a specific object in a specific way using monocular RGB images from a gripper camera.

The question we address in this work is whether it is possible to learn an end-to-end policy to grasp a specific object from a specific direction using an RGB camera-in-hand. Further we also investigate whether this policy can be learned using simulation only. Simulation has the potential to unlock new robotic learning approaches by generating an almost unlimited amount of training data, essentially for free. To train a policy that overcomes the *reality gap* problem (*i.e.*, the mismatch between simulated and real distributions), we have developed a simulation environment with the following design criteria, see Fig. 1: 1) it models physical contact, 2) it generates photorealistic images for training policies based on RGB alone, and 3) it supports domain randomization to facilitate invariance to various lighting conditions and background textures.

Our contributions are thus:

- A deep reinforcement learning (RL) approach to *directional semantic grasping* that learns to grasp specific objects along specific grasp directions in an end-to-end fashion from RGB images from an in-hand camera.
- A robotic simulator that generates physically plausible, photorealistic synthetic data, with contact modeling and domain randomization, to train policies that transfer to the real world without a special domain adaptation step.

- A system that combines the learned camera-in-hand policies for local control with global 6-DoF pose estimation [6] from a fixed camera in order to grasp objects anywhere in the graspable workspace.

## II. PREVIOUS WORK

**Robotic grasping** is fundamental to pick-and-place tasks and has been studied by a number of researchers. Dex-Net [1], [2], [4], [3] is a deep network aimed at indiscriminate top-down grasping of objects in a bin using an overhead depth camera; the network is trained entirely in simulation. In contrast, the approach of Levine *et al.* [7] learns an indiscriminate top-down grasp prediction model from an overhead RGB camera using hundreds of thousands of grasp attempts by a collection of real robots. Jang *et al.* [5] address the problem of semantic grasping, in which a two-stream network learns top-down grasps of specific classes of objects, trained on tens of thousands of manually-labeled real RGB images and hundreds of thousands of images utilizing self-supervised label propagation. Morrison *et al.* [8] learn a mapping from a wrist-mounted depth image to the quality and pose of grasps at every pixel, trained on labeled real depth images. Morrison *et al.* [9] combine RGB pixelwise semantic segmentation with depth sensing for multimodal top-down semantic grasping. Quillen *et al.* [10] compare a variety of off-policy deep RL methods for indiscriminate top-down grasping using purely simulated data for both training and test.

**Domain adaptation** aims to allow a network trained on simulated data to generalize to real data, using some amount of labeled real data. Various researchers have explored ways to reduce the amount of labeled real data needed. Fang *et al.* [11] address top-down grasping of household dishes from instance-segmented images from a wrist-mounted RGB camera; sim-to-real transfer is accomplished using multi-task domain adaptation with real indiscriminate grasping data. Bousmalis *et al.* [12] present a GAN-based domain adaptation model for sim-to-real transfer for top-down indiscriminate grasping using a monocular RGB camera. Zhang *et al.* [13] propose an adversarial discriminative transfer approach to reduce the amount of labeled real data required for sim-to-real transfer for the task of reaching a blue cube using an RGB camera and an end-to-end network. Sadeghi *et al.* [14] use an auxiliary adaptation loss to finetune the perception layers of a neural network using a small amount of annotated real data, to solve the problem of viewpoint-invariant visual servoing to reach a desired object.

**Sim-to-real transfer without domain adaptation** is the ambitious goal of training in simulation and executing in the real world without any labeled real-world data. James *et al.* [15] learn an end-to-end policy entirely in simulation to grasp a red cube and place it inside a blue basket using RGB images; sim-to-real transfer is accomplished via domain randomization. Similarly, Matas *et al.* [16] train an end-to-end deep RL policy in simulation to manipulate deformable objects using RGB images; domain randomization is used to cross the reality gap. Yan *et al.* [17] use imitation learning

to grasp a tiny yellow sphere from RGB images by training a network to perform a binary segmentation of the sphere from the background.

The transfer is easier when performed purely with depth images, although this prevents the network from using valuable visual information, and it requires less standard hardware with additional error modes. Vierech *et al.* [18] learn a visuomotor controller for indiscriminate top-down grasping using a wrist-mounted depth sensor, trained in simulation. Osa *et al.* [19] use hierarchical RL to autonomously collect a simulated grasping dataset for learning grasping strategies for isolated objects from depth images; the system is capable of grasping from multiple angles. Fang *et al.* [20] use self-supervision to generate simulated data for learning task-oriented grasping for tool manipulation from depth images.

**Object manipulation** broadly encompasses pick-and-place tasks of known objects in the robot workspace. The MOPED framework [21] performs real-time detection and pose estimation of multiple known objects from one or more RGB images for the purpose of object manipulation. SimTrack [22] is a framework for real-time detection and tracking of multiple known objects using combined RGBD/RGB (overhead/in-hand) sensors, for the purpose of grasping, manipulating, and stacking objects in a tabletop environment. Sui *et al.* [23] address the problem of axiomatic scene estimation for goal-directed top-down manipulation of rigid objects on a table, using an RGBD sensor. Zeng *et al.* [24] uses a 2D object detector and depth sensing to find the poses of known objects in a tabletop scene using an RGBD sensor, and motion planning for grasping and manipulation.

Since our goal is also sim-to-real transfer of an end-to-end policy trained on simulated RGB images without any labeled real data, our work is most similar to that of James *et al.* [15] and Matas *et al.* [16] above. Like their approaches, we also use domain randomization to bridge the reality gap. Our work differs in our use of a simulator that models physical contact and generates photorealistic imagery for learning to map images of textured objects to actions that aim to grasp specific objects from specific angles.

## III. METHOD

Adopting the standard reinforcement learning formulation, we model the problem as a partially observable Markov decision process (POMDP) represented as a tuple  $(S, O, A, P, r, \gamma)$ , where  $S$  is the set of states in the environment,  $O$  is the set of observations (*i.e.*, downsampled RGB images from the wrist-mounted camera),  $A$  is the set of actions (*i.e.*, end-effector-centric 3D Cartesian motion and rotation about the wrist axis),  $P : S \times A \times S \rightarrow \mathbb{R}$  is the state transition probability function,  $r : S \times A \rightarrow \mathbb{R}$  is the reward function, and  $\gamma$  is a discount factor.

The goal of training is to learn a deterministic policy  $\pi : O \rightarrow A$  such that taking action  $a_t = \pi(o_t)$  at time  $t$  maximizes the sum of discounted future rewards from state  $s_t$ :  $R_t = \sum_{i=t}^{\infty} \gamma^{i-t} r(s_i, a_i)$ . After taking action  $a_t$ , the environment transitions from state  $s_t$  to state  $s_{t+1}$  by

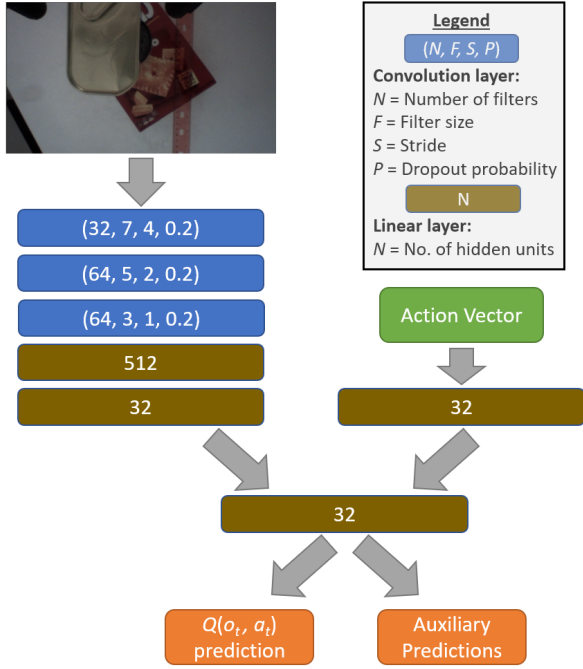


Fig. 2. Detailed network structure: The RGB image from the gripper camera is embedded by a deep neural network. This embedding is then concatenated with the action vector (after a single linear layer) to an additional layer to estimate the Q-value, as well as auxiliary targets. Both the Q-value loss and auxiliary losses are used during training.

sampling from  $P$ . The quality of taking action  $a_t$ , given observation  $o_t$  is measured by  $Q(o_t, a_t) = \mathbb{E}[R_t|o_t, a_t]$ , known as the  $Q$ -function.

In our environment, each action  $a_t = (\delta x_t, \delta y_t, \delta z_t, \delta \phi_t)$  has 4 degrees of freedom, where  $(\delta x_t, \delta y_t, \delta z_t) \in [-\Delta_{tran}, \Delta_{tran}]^3$  denotes the translation of the gripper (in the gripper coordinate frame), and  $\delta \phi_t \in [-\Delta_{rot}, \Delta_{rot}]$  denotes the change in rotation of the gripper about its longitudinal axis; where we set the maximum translation and rotation to  $\Delta_{tran} = 5$  cm and  $\Delta_{rot} = \pi/4$  rad, respectively. Note that since the action is relative to the gripper, rather than in the world coordinate frame, the system is agnostic to the absolute orientation of the object being grasped. Each observation  $o_t \in \mathbb{R}_+^{w \times h \times 3}$  is an RGB image from the camera in hand, with  $w = 64, h = 40$ .

Recent work in reinforcement learning has extended classic approaches to complex observation spaces (e.g., images) [25] and continuous action spaces (e.g., robot velocities) [26] using deep neural networks as function approximators for  $Q(o_t, a_t)$  and/or  $\pi(o_t)$ . In this work, we use Deep Q-learning (DQN) [25], an off-policy, model-free RL algorithm, which only requires learning one network (the  $Q$ -function). Specifically, we use a double deep  $Q$ -network (DDQN) [27], which overcomes an important limitation of DQN (namely, the overestimation of action values) by using separate networks for action selection and action evaluation, copying the weights from one to the other periodically.

As shown in Fig. 2, the learned  $Q$ -function maps a downsampled  $64 \times 40$  RGB image from the camera mounted

on the wrist of the robot as well as a continuous 4D value representing an action in the end-effector-centric Cartesian coordinate system to a single scalar value,  $Q(o_t, a_t)$ . Gripper images and actions are processed separately (using a convolutional net with dropout [28] for the former and a single linear layer for the latter) before concatenating their intermediate representations into a single vector that is fed through a linear layer and then split into two output layers: one for predicting  $Q$ -values and another for predicting auxiliary targets. Rectified Linear Units (ReLUs) are used for nonlinearity throughout the network. The auxiliary targets are heuristically selected features correlated with rewards for improving the learning signal available to the network. We use the following two quantities as auxiliary targets: 1) distance of the gripper to the centroid of the current object, and 2) the rotational offset of the gripper with respect to the object. Mean squared error is used as the loss function for both.

Since  $Q$ -learning requires selecting the action with the highest  $Q$ -value, and since our action space is continuous, this maximum needs to be approximated. We adopt the approach of prior work [7], [5], [10] by using the cross-entropy method (CEM) [29] to select the best action. This process consists of randomly sampling  $n_a$  actions from a multivariate Gaussian distribution (with diagonal covariance), evaluating their  $Q$ -values, selecting the best  $n_b$  actions, refitting the sampling distribution to these actions, and iterating the procedure  $n_n$  times until convergence, upon which the mean of the distribution is output as the best action. Despite being an approximation, this approach works well in practice for low-dimensional action spaces. (During training,  $n_a = 16$ ,  $n_b = 5$ , and  $n_n = 2$ ; during testing,  $n_a = 64$ ,  $n_b = 6$ , and  $n_n = 3$ .)

Training is performed entirely off-policy using a dataset of grasps collected with a pseudo-random policy that moves with a bias toward the object being grasped. This paradigm allows us to train and evaluate many different types of models without requiring new rollouts in simulation, which are time-consuming to collect.

During training, domain randomization [30] is applied to bridge the reality gap. Specifically, random textures are applied to the table, as shown in Fig. 3, to assist the learned model to be invariant to various backgrounds and distractions. Similarly, each image's hue, saturation, and brightness is randomized. Additionally, we apply random Gaussian blur to the image (with kernel size uniformly selected from 1.0 to 3.0 pixels), in order to prevent overfitting to texture details in the object models that may vary from simulation to reality.

During training, the initial position of the gripper is randomized to be within a  $5 \times 5$  cm area at a height between 2 and 4.5 cm above the top of the object, with rotation offset from the desired object grasping position by as much as  $\pm \pi/4$  radians. These conditions were selected conservatively based on the error observed by our pose estimation algorithm [6] to enable grasping anywhere in the workspace. From an initial position/orientation, the robot moves  $k = 5$  time steps before attempting to grasp and lift



Fig. 3. Domain randomization, including random table texture, is used to make the network robust to changes in the visual input. Training time is reduced by running multiple simulated robots in parallel.

the object. The reward function gives a positive reward for a successful grasp at the end of an episode (*i.e.*, object is held by the gripper after the lift is performed), a negative penalty for distance to the centroid of the object, and a negative penalty for displacing the object prior to attempting a grasp.

Note that, during training, the tips of the parallel-jaw gripper interact with the object according to the underlying physics engine. That is, the object is grasped and lifted only if there is sufficient force between the tips of the fingers to keep the object in place. This is unlike previous work that either assumes that the object is grasped if the gripper is below some threshold in height [10], or that uses analytic grasp calculations to estimate whether the grasp is successful [2]. However, we discovered that the model learned to exploit a deficiency in the physics engine of our simulator, whereby it presses its gripper down on top of the object (rather than fit around it as desired), and the gripper would eventually snap into place around the object. As this behavior does not match the real world, due to the rigidity of the objects, we found it necessary to avoid this behavior by inserting an additional reward penalty on contact forces against the tips of the gripper’s fingers prior to attempting a grasp.

#### IV. ROBOTIC SIMULATOR

Two key components of a robotic simulator are its fidelity in modeling the physics of the world, and its fidelity in producing realistic sensory data. Although existing physical simulators [31], [32], [33] have made significant strides toward both of these goals, there is much room for progress. In particular, photorealistic camera imagery and detailed contact modeling are two features that are missing from most off-the-shelf simulators. Below we describe our progress toward achieving these goals. For an alternate approach, see [34], and for a comparison of various simulation tools, see [35].

We have developed our own robotic simulator built on Unreal Engine 4 (UE4). UE4 is a highly customizable game engine with state-of-the-art rendering capabilities. UE4 has well established scene editing workflows and scripting tools, an active marketplace with a variety of 3D assets, procedural textures, rendering plugins, and a thriving developer

community. The simulator is agnostic to the underlying physics solver, with two options currently integrated: PhysX<sup>2</sup> and FleX<sup>3</sup>. PhysX models rigid bodies, whereas FleX is a GPU-based particle simulation library designed for real-time applications such as rigid body stacking, particle piles, soft bodies, and fluids. Both solvers allow the modeling of contact forces for object/robot interactions.

The simulator communicates with a controller using an efficient cross-application messaging system. This decoupling enables control code to switch between interacting with the simulator and real robot with minimal change. The robot is controlled using either joint trajectories, velocities, accelerations, or forces through a configurable PID controller. Specific sensors such as force, depth images, RGB images, object segmentation, object poses, 2D bounding boxes, and 3D cuboids can be added/subscribed. At runtime, the scene can be modified such as changing the poses of object(s), camera(s) and/or robot(s). Physical objects in the simulator are represented using URDF which facilitates the introduction of new robots or objects. The simulator is designed for fast iterations and easy experimentation, by making the physics engines switchable at runtime, simplifying URDF import to dragging and dropping the file, and other facilities to emphasize ease of use. In addition, the simulator includes domain randomization tools such as randomizing textures, lights, colours, and object physical properties, to facilitate sim-to-real transfer.

#### V. EXPERIMENTAL RESULTS

To evaluate the proposed approach, we performed a series of experiments both in simulation and in the real world. The evaluation in simulation was performed on a held-out environment with lighting and textures remaining consistent throughout the experiments, as opposed to the highly randomized environment seen in the training data.

All experiments were conducted with a Baxter robot (either in simulation or in reality). The Baxter has a simple parallel jaw gripper at the end effector, capable of traveling a total of approximately 4 cm between the two fingers. The camera is mounted in the wrist aimed parallel to the fingers, producing  $640 \times 400$  images at 30 Hz.

##### A. Simulation

We used the procedure described earlier to train a network using four different objects from the YCB dataset [36], [37]: meat can, soup can, sugar box, and mustard bottle. These objects were chosen to cover a variety of geometric shapes (rounded cuboid, cylinder, squared cuboid, and a unique curved shape), material properties (matte, reflective), and colors (brightly colored, dark). They were also selected because detection/pose estimation networks for them are already available [6]. For all objects, two models were trained: one for grasping the top of the object (top-down) and another for grasping from all directions (multi-side). More specifically, for all but the soup can, the multi-side

<sup>2</sup><https://developer.nvidia.com/physx-sdk>

<sup>3</sup><https://developer.nvidia.com/flex>

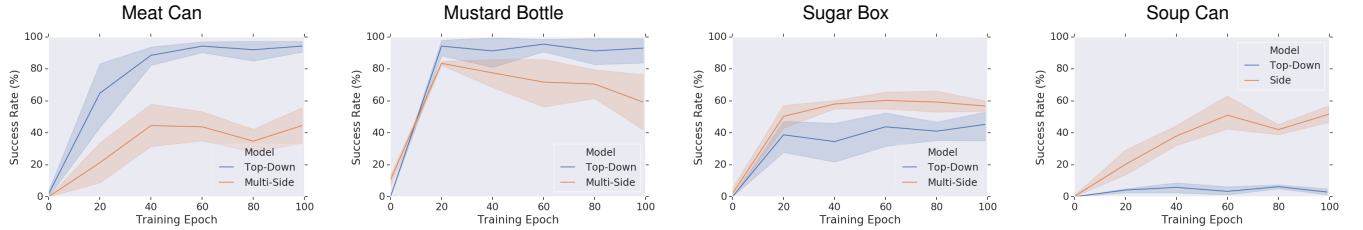


Fig. 4. Grasp success rate, evaluated on a simulated held-out environment, over the course of training for the four different YCB models. Shown are results for top-down grasping as well as grasping from multiple sides (either the top or the two graspable sides).

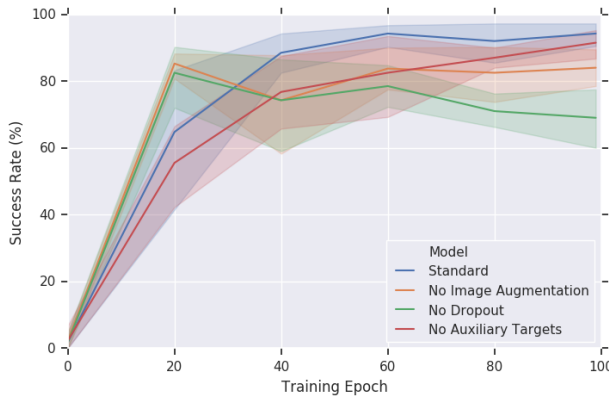


Fig. 5. Ablation study with top-down grasping of the meat can, trained with various components missing.



Fig. 6. After training in simulation, the policy is able to grasp the intended object in the real world without fine-tuning. Because the action space is gripper-centric, the robot is capable of grasping from various orientations, such as vertical (left) and horizontal (right). Gripper images used as input to the method are shown as insets.

models were trained with data from all three directions (top and the two graspable sides) so that they are capable of grasping from either the top or two side directions; whereas the soup can was trained to grasp from any of its infinite side grasping directions. All models were trained with 100,000 data samples each.

Training results are shown in Fig. 4. Both the meat can and mustard bottle achieved 95% success or more with the top-down grasp models, and reasonable success at multi-side grasping. With the sugar box, results are inverted, with the multi-side version performing better than top-down. This inversion is due to the lack of texture on the white top of the box, coupled with the fact that the held-out environment used for evaluation consisted of a light-colored table. The soup can achieved reasonable success for side grasping, but top-down grasping proved to be challenging in simulation due to the gripper's tendency to slip off the curved surface from incorrect friction modeling.

TABLE I  
GRASP SUCCESS RATE OF VARIOUS OBJECTS IN THE REAL WORLD,  
AFTER TRAINING ONLY IN SIMULATION.

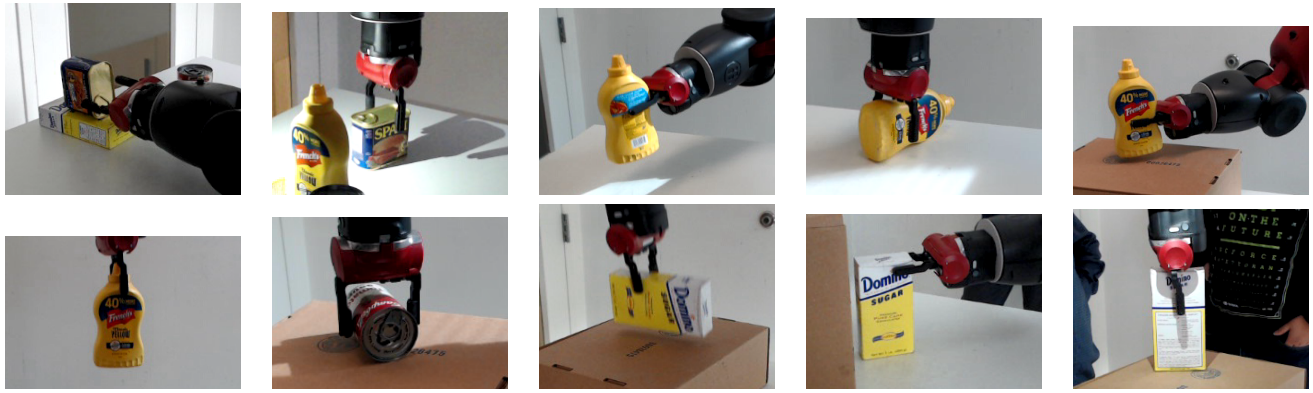
object	grasp success (%) top	multi-side
meat can	83.3	75.0
mustard bottle	100.0	66.7
sugar box	50.0	66.7
soup can	33.3	50.0

An ablation study was performed to evaluate the effectiveness of specific components on successful training. These components were isolated and removed, and the resulting performance was then measured. The results of this ablation study are shown in Fig. 5 for the top-down meat can model; other objects are similar. From this experiment we see that, without image augmentation, the model improves quickly but then reaches a maximum, after which it declines in performance due to overfitting. Behavior without dropout was similar, with an even more pronounced effect. Thus we see that both image augmentation and dropout are important for good results. Similarly, auxiliary targets improve overall performance slightly while it reduces training time significantly.

### B. Real world

To quantify the performance in the real world, we placed the YCB objects at various places on a table. Due to the poor quality of the in-hand Baxter camera, we had to manually adjust the gain of the camera; and the room lighting was also adjusted to reduce the effects of reflections that are not modeled in simulation. The grasp success rate, starting from a manual pre-grasp above the object in roughly the same area as in simulation, is shown in Tab. I. These results show that the network successfully learned policies that transfer to the real world under challenging conditions. As expected, the soup can performs better on side grasps than top grasps. The mustard bottle is the reverse, with top grasps being easier than side grasps. Note that top-down grasping of the soup is better in the real-world than simulation due to the increased friction in the real world that yields more forgiving behavior when the can is grasped off-center.

Fig. 6 shows two examples of the policy learned in simulation successfully grasping an object in the real world. Shown in the image are top-down grasps from both a vertical and horizontal direction, in a cluttered environment, showing



(a) Grasping of various objects from different directions by real Baxter robot.



(b) Corresponding images from the wrist-mounted camera.

Fig. 7. Additional experiments showing the ability of the robotic system to grasp the meat can, mustard bottle, soup can, and sugar box in the real-world, after being trained only in simulation. Note the variety of top-down and side grasps, as well as lighting conditions and backgrounds.

the versatility of wrist-centric control.

Additional real-world experiments are shown in Fig. 7. The system is capable of grabbing the four objects on which it was trained from various directions (side and top). Note the variety of lighting conditions, including dark and bright images, with and without specular highlights. Nevertheless, one difficulty we encountered is the lack of material properties in our object models. As a result, the metallic top of the meat can causes specular reflections in reality that are not present in the simulated images, as also noted in [6]. Though our approach is able to ignore small reflections, more accurate models in simulation would alleviate this problem.

We also integrated our approach into a system that uses deep object pose estimation (DOPE) [6] to detect and estimate the 6-degree-of-freedom (6-DoF) pose of objects using a chest-mounted RGB camera. Like the approach described in this paper, DOPE was trained only on simulated data without fine-tuning, using a combination of domain randomization and photorealistic synthetic data to bridge the reality gap. The 6-DoF pose is used to move the end effector to a pre-grasp.

If the pose estimation, calibration, and motion control were all accurate, then simple open-loop control would yield a successful grasp. In practice, however, all three of these aspects of the solution contribute error to the open-loop motion. As a result, such an approach sometimes fails to grasp the object. The purpose of our deep RL approach is to leverage closed-loop control to enable the robot to recover

from pre-grasp errors and adjust to disturbances in either pose estimation, extrinsic calibration, or motion control.

## VI. CONCLUSION

In this paper we have explored the problem of end-to-end learning of directional semantic grasping of household objects. We have developed a robotic simulator that models physical reality (including contact) and is capable of capturing photorealistic training data, while at the same time supporting domain randomization. Using this simulator we trained a network, using the deep RL algorithm of DDQN, to learn to grasp a set of household objects from specific directions in a closed-loop fashion from RGB images. To alleviate the errors associated with extrinsic camera calibration or other factors, the system uses a camera-in-hand. The combination of physical realism, photorealism, and domain randomization enables the network to run in the real world without further adaptation. The system was tested on a real Baxter robot showing promising results of such an approach for real-world applications. For future work, we plan to explore further the robustness of the proposed method by expanding the set of objects, increasing robustness to robot initial poses and extreme lighting conditions, improving contact and friction modeling, including temporal information, and increasing the number of objects.

## ACKNOWLEDGMENTS

We thank Stephen Tyree, Iuri Frosio, Ryan Oldja, and Abhishek Raj Dutta for their help with the project.

## REFERENCES

[1] J. Mahler, F. T. Pokorny, B. Hou, M. Roderick, M. Laskey, M. Aubry, K. Kohlhoff, T. Kröger, J. Kuffner, and K. Goldberg, “Dex-Net 1.0: A cloud-based network of 3D objects for robust grasp planning using a multi-armed bandit model with correlated rewards,” in *IEEE International Conference on Robotics and Automation (ICRA)*, 2016, pp. 1957–1964.

[2] J. Mahler, J. Liang, S. Niyaz, M. Laskey, R. Doan, X. Liu, J. A. Ojea, and K. Goldberg, “Dex-Net 2.0: Deep learning to plan robust grasps with synthetic point clouds and analytic grasp metrics,” in *Robotics: Science and Systems (RSS)*, 2017.

[3] J. Mahler and K. Goldberg, “Learning deep policies for robot bin picking by simulating robust grasping sequences,” in *Proceedings of the 1st Annual Conference on Robot Learning (CoRL)*, 2017, pp. 515–524.

[4] J. Mahler, M. Matl, X. Liu, A. Li, D. Gealy, and K. Goldberg, “Dex-Net 3.0: Computing robust robot suction grasp targets in point clouds using a new analytic model and deep learning,” in *IEEE International Conference on Robotics and Automation (ICRA)*, 2018.

[5] E. Jang, S. Vijaynarasimhan, P. Pastor, J. Ibarz, and S. Levine, “End-to-end learning of semantic grasping,” in *CoRL*, 2017.

[6] J. Tremblay, T. To, B. Sundaralingam, Y. Xiang, D. Fox, and S. Birchfield, “Deep object pose estimation for semantic robotic grasping of household objects,” in *CoRL*, 2018.

[7] S. Levine, P. Pastor, A. Krizhevsky, J. Ibarz, and D. Quillen, “Learning hand-eye coordination for robotic grasping with deep learning and large-scale data collection,” *The International Journal of Robotics Research (IJRR)*, vol. 37, no. 4–5, pp. 421–436, 2018.

[8] D. Morrison, P. Corke, and J. Leitner, “Closing the loop for robotic grasping: A real-time, generative grasp synthesis approach,” in *RSS*, 2018.

[9] D. Morrison, A. W. Tow, M. McTaggart, R. Smith, N. Kelly-Boxall, S. Wade-McCue, J. Erskine, R. Grinover, A. Gurman, T. Hunn, D. Lee, A. Milan, T. Pham, G. Rallo, A. Razjigaev, T. Rowntree, K. Vijay, Z. Zhuang, C. Lehner, I. Reid, P. Corke, and J. Leitner, “Cartman: The low-cost Cartesian manipulator that won the Amazon Robotics Challenge,” in *ICRA*, 2018.

[10] D. Quillen, E. Jang, O. Nachum, C. Finn, J. Ibarz, and S. Levine, “Deep reinforcement learning for vision-based robotic grasping: A simulated comparative evaluation of off-policy methods,” in *ICRA*, 2018.

[11] K. Fang, Y. Bai, S. Hinterstoisser, and M. Kalakrishnan, “Multi-task domain adaptation for deep learning of instance grasping from simulation,” in *arXiv:1710.06422*, 2017.

[12] K. Bousmalis, A. Irpan, P. Wohlhart, Y. Bai, M. Kelcey, M. Kalakrishnan, L. Downs, J. Ibarz, P. Pastor, K. Konolige, S. Levine, and V. Vanhoucke, “Using simulation and domain adaptation to improve efficiency of deep robotic grasping,” in *ICRA*, 2018.

[13] F. Zhang, J. Leitner, Z. Ge, M. Milford, and P. Corke, “Adversarial discriminative sim-to-real transfer of visuo-motor policies,” in *arXiv:1709.05746*, 2017.

[14] F. Sadeghi, A. Toshev, E. Jang, and S. Levine, “Sim2Real viewpoint invariant visual servoing by recurrent control,” in *Proceedings of the IEEE Conference on Computer Vision and Pattern Recognition (CVPR)*, 2018, pp. 4691–4699.

[15] S. James, A. J. Davison, and E. Johns, “Transferring end-to-end visuomotor control from simulation to real world for a multi-stage task,” in *CoRL*, 2017.

[16] J. Matas, S. James, and A. J. Davison, “Sim-to-real reinforcement learning for deformable object manipulation,” *arXiv:1806.07851*, 2018.

[17] M. Yan, I. Frosio, S. Tyree, and J. Kautz, “Sim-to-real transfer of accurate grasping with eye-in-hand observations and continuous control,” in *NIPS Workshop on Acting and Interacting in the Real World: Challenges in Robot Learning*, 2018.

[18] U. Viereck, A. ten Pas, K. Saenko, and R. Platt, “Learning a visuomotor controller for real world robotic grasping using simulated depth images,” in *CoRL*, 2017.

[19] T. Osa, J. Peters, , and G. Neumann, “Experiments with hierarchical reinforcement learning of multiple grasping policies,” in *ISER*, 2016.

[20] K. Fang, Y. Zhu, A. Garg, A. Kurenkov, V. Mehta, L. Fei-Fei, and S. Savarese, “Learning task-oriented grasping for tool manipulation from simulated self-supervision,” in *RSS*, 2018.

[21] A. Collet, M. Martinez, and S. S. Srinivasa, “The MOPED framework: Object recognition and pose estimation for manipulation,” *International Journal of Robotics Research*, vol. 30, no. 10, pp. 1284–1306, 2011.

[22] K. Pauwels and D. Kragic, “SimTrack: A simulation-based framework for scalable real-time object pose detection and tracking,” in *IROS*, 2015.

[23] Z. Sui, L. Xiang, O. C. Jenkins, and K. Desingh, “Goal-directed robot manipulation through axiomatic scene estimation,” *International Journal of Robotics Research (IJRR)*, vol. 36, no. 1, pp. 86–104, 2017.

[24] Z. Zeng, Z. Zhou, Z. Sui, and O. C. Jenkins, “Semantic robot programming for goal-directed manipulation in cluttered scenes,” in *ICRA*, 2018.

[25] V. Mnih, K. Kavukcuoglu, D. Silver, A. A. Rusu, J. Veness, M. G. Bellemare, A. Graves, M. Riedmiller, A. K. Fidjeland, G. Ostrovski, S. Petersen, C. Beattie, A. Sadik, I. Antonoglou, H. King, D. Kumaran, D. Wierstra, S. Legg, and D. Hassabis, “Human-level control through deep reinforcement learning,” *Nature*, vol. 518, pp. 529–533, 2015.

[26] T. P. Lillicrap, J. J. Hunt, A. Pritzel, N. Heess, T. Erez, Y. Tassa, D. Silver, and D. Wierstra, “Continuous control with deep reinforcement learning,” in *ICLR*, 2016.

[27] H. van Hasselt, A. Guez, and D. Silver, “Deep reinforcement learning with double Q-learning,” in *AAAI*, 2016.

[28] N. Srivastava, G. Hinton, A. Krizhevsky, I. Sutskever, and R. Salakhutdinov, “Dropout: A simple way to prevent neural networks from overfitting,” *The Journal of Machine Learning Research*, vol. 15, no. 1, pp. 1929–1958, 2014.

[29] P.-T. De Boer, D. P. Kroese, S. Mannor, and R. Y. Rubinstein, “A tutorial on the cross-entropy method,” *Annals of Operations Research*, vol. 134, no. 1, pp. 19–67, 2005.

[30] J. Tobin, R. Fong, A. Ray, J. Schneider, W. Zaremba, and P. Abbeel, “Domain randomization for transferring deep neural networks from simulation to the real world,” in *IROS*, 2017.

[31] T. E. Emanuel Todorov and Y. Tassa, “MuJoCo: A physics engine for model-based control,” in *IROS*, 2012.

[32] E. Rohmer, S. P. N. Singh, and M. Freese, “V-REP: A versatile and scalable robot simulation framework,” in *IROS*, 2013.

[33] E. Coumans and Y. Bai, “PyBullet: A Python module for physics simulation in robotics, games and machine learning,” 2017. [Online]. Available: <http://pybullet.org>

[34] A. Juliani, V.-P. Berges, E. Vckay, Y. Gao, H. Henry, M. Mattar, and D. Lange, “Unity: A general platform for intelligent agents,” in *arXiv:1809.02627*, 2018.

[35] T. Erez, Y. Tassa, and E. Todorov, “Simulation tools for model-based robotics: Comparison of Bullet, Havok, MuJoCo, ODE and PhysX,” in *ICRA*, 2015.

[36] B. Calli, A. Walsman, A. Singh, S. Srinivasa, P. Abbeel, and A. M. Dollar, “The YCB object and model set: Towards common benchmarks for manipulation research,” in *Intl. Conf. on Advanced Robotics (ICAR)*, 2015.

[37] ———, “Benchmarking in manipulation research: Using the Yale-CMU-Berkeley object and model set,” *IEEE Robotics and Automation Magazine*, vol. 22, no. 3, Sept. 2015.